Common alterations in PBP1a from resistant streptococcus pneumoniae decrease its reactivity towards beta -lactams: Structural insights.

Viviana Job, Raphaël Carapito, Thierry Vernet, Andréa Dessen, André Zapun

THE JOURNAL OF BIOLOGICAL CHEMISTRY VOL. 283, NO. 8, pp. 4886–4894, February 22, 2008

Common Alterations in PBP1a from Resistant *Streptococcus pneumoniae* Decrease Its Reactivity toward β-Lactams

STRUCTURAL INSIGHTS[*][S]

Received for publication, July 27, 2007, and in revised form, October 19, 2007 Published, JBC Papers in Press, November 30, 2007, DOI 10.1074/jbc.M706181200

Viviana Job[‡], Raphaël Carapito[§], Thierry Vernet[§], Andréa Dessen[‡], and André Zapun[§1]

From the [‡]Laboratoire des Protéines Membranaires and the [§]Laboratoire d'Ingénierie des Macromolécules, Institut de Biologie Structurale Jean-Pierre Ebel, Université Joseph Fourier, UMR 5075-CNRS, CEA Grenoble, France

The development of high level β-lactam resistance in the pneumococcus requires the expression of an altered form of PBP1a, in addition to modified forms of PBP2b and PBP2x, which are necessary for the appearance of low levels of resistance. Here, we present the crystal structure of a soluble form of PBP1a from the highly resistant *Streptococcus pneumoniae* strain 5204 (minimal inhibitory concentration of cefotaxime is 12 mg·liter^{-1}). Mutations T371A, which is adjacent to the catalytic nucleophile Ser^{370}, and TSQF(574–577)NTGY, which lie in a loop bordering the active site cleft, were investigated by site-directed mutagenesis. The consequences of these substitutions on reaction kinetics with β-lactams were probed *in vitro*, and their effect on resistance was measured *in vivo*. The results are interpreted in the framework of the crystal structure, which displays a narrower, discontinuous active site cavity, compared with that of PBP1a from the β-lactam susceptible strain R6, as well as a reorientation of the catalytic Ser^{370}.

Clinical isolates of *Streptococcus pneumoniae* are now often resistant to multiple drugs. In France, where the problem is particularly significant, ~50% of the isolates have decreased susceptibility to β-lactams, most often combined with resistance to other classes of antibiotics such as erythromycin, tetracyclines, or sulfonamides (1).

β-Lactams interfere with the formation of peptidoglycan, an essential component of the cell wall, by inhibiting the transpeptidation reaction that cross-links peptidoglycan stem peptides. This reaction, catalyzed by penicillin-binding proteins (PBPs),[2] is essential for the stability of the cell wall. The formation of long-lived covalent adducts by β-lactam antibiotics within the PBP active site results in growth arrest or cell death (2). Studies of the mechanisms of pneumococcal resistance to β-lactams have been performed for the past two decades through the employment of techniques ranging from epidemiological to structural analyses, and have converged on a common fact: *S. pneumoniae* resists β-lactams by introducing amino acid substitutions into key PBPs, which have then a decreased affinity for these antibiotics (3). The altered enzymes retain nonetheless their physiological activities. Of the six pneumococcal PBPs, three are modified in most resistant strains: PBP2b, PBP2x, and PBP1a (4–6). These low-affinity PBPs are encoded by mosaic genes that combine sequence fragments from various origins, including closely related species such as *Streptococcus mitis* and *Streptococcus oralis* (7, 8). Although the geographic extent of resistance has been attributed to the spread of a small number of initial clones (9), the genetic plasticity is such that several dozen of different sequences have now been documented for the three low-affinity PBPs. Examination of the sequences and crystal structures of PBP2x variants have revealed the existence of at least two distinct mechanisms for reducing the affinity of this enzyme for β-lactams (10). The transpeptidase (TP) domains of low-affinity PBPs typically contain between 20 and 40 amino acid substitutions (when compared with PBPs from the β-lactam-susceptible R6 strain). Many of the substitutions are likely irrelevant to the resistance mechanism, as they have been imported through homologous recombination with mutations that truly decrease the affinity for β-lactams. We have shown recently that out of 41 substitutions in PBP2x from the highly resistant strain 5204, only 6 contribute significantly to lowering the affinity for β-lactams (11).

PBP2b and PBP2x are often referred to as primary determinants of β-lactam resistance, because cultivation of pneumococci in the presence of low amounts of piperacillin or cefotaxime selects for mutations in PBP2b or PBP2x, respectively (12). However, the levels of resistance conferred by low-affinity PBP2b and/or PBP2x variants are limited by the inhibition of the other unmodified PBPs. High levels of resistance are achieved only upon further alteration of PBP1a (13–16). Low-affinity PBP1a is therefore the most troublesome PBP from a clinical point of view.

PBP1a is a bifunctional, class A enzyme, in that it consists of a short cytoplasmic region, an N-terminal membrane anchor

* This work was funded by the COBRA grant from the 6th European Framework Program (COBRA LSHM-CT-2003-503335). The costs of publication of this article were defrayed in part by the payment of page charges. This article must therefore be hereby marked "*advertisement*" in accordance with 18 U.S.C. Section 1734 solely to indicate this fact.

The atomic coordinates and structure factors (code 2V2F) have been deposited in the Protein Data Bank, Research Collaboratory for Structural Bioinformatics, Rutgers University, New Brunswick, NJ (http://www.rcsb.org/).

[S] The on-line version of this article (available at http://www.jbc.org) contains supplemental data and Figs. S1 and S2.

[1] To whom correspondence should be addressed: Institut de Biologie Structurale, 41 rue Jules Horowitz, 38025 Grenoble, France. Tel.: 33-4-38-78-92-03; Fax: 33-4-38-78-54-94; E-mail: andre.zapun@ibs.fr.

[2] The abbreviations used are: PBP, penicillin-binding protein; TP, transpeptidase; GT, glycosyltransferase; CTX, cefotaxime; penG, penicillin G; MES, 2-morpholinoethanesulfonic acid; r.m.s., root-mean-square; GST, glutathione *S*-transferase; PEG, polyethyleneglycol.

segment, followed by a glycosyltransferase domain (GT), a linker region and a TP domain (17). The crystal structure of a soluble, proteolyzed form of PBP1a from strain R6 reveals that the TP domain, whose fold is typical of the serine penicilloyl transferase family of enzymes, is flanked by a short C-terminal region and an N-terminal β-strand-rich region, which carries a small peptide of the glycosyltransferase domain and serves as a linker between the two catalytic units (18).

Among 47 publicly available different sequences representing the TP domains from PBP1a variants (residues 264–654), 7 are very similar to the sequence of PBP1a from strain R6 with 1 to 4 amino acid substitutions. In contrast, 39 sequences are clearly mosaic and are presumably all from strains with reduced susceptibility to β-lactams. They carry between 13 and 60 substitutions over the entire TP domain. Individual reversion of the substitutions in PBP1a from strain 3191 (19), which harbors 52 mutations in the TP domain, reduced the level of resistance in only two cases: a L539W substitution that is present in only two sequences, and the TSQF to NTGY substitutions at positions 574–577, which are present in nearly all mosaic sequences (38 out of 39).

Here we present the crystal structure of a soluble form of PBP1a from the highly resistant pneumococcal strain 5204 (MIC_{penG} = 6.0 mg·liter^{-1}; MIC_{CTX} = 12.0 mg·liter^{-1}) (20). This PBP1a carries 48 substitutions when compared with the R6 strain, including 45 within the TP domain. The reaction between penicillin G and cefotaxime, and four different PBP1a clinical variants, as well as point mutants in positions 574–577, were also studied. The impact of these PBP1a variants on resistance was measured. The results are interpreted within the framework of the crystal structures of PBP1a from strains R6 and 5204.

EXPERIMENTAL PROCEDURES

Plasmids and Site-directed Mutagenesis—Pneumococcal strains 4790, 5204, 5245, 5259 (University Hospital, Grenoble, France), and R6 were used as sources of genomic DNA for the amplification of *pbp1a* genes. The fragments encoding the extracellular region of PBP1a (residues 37–719, henceforth noted PBP1a) were PCR-amplified and introduced as BamHI/XhoI fragments in place of the *pbp2x* fragment in pGEX-S-pbp2x*-f1 (21). This vector had been previously modified by site-directed mutagenesis to eliminate a second undesired BamHI site (GGATCC into GGGTCC) in the f1 region.

Site-directed mutagenesis of *pbp1a* genes from strains R6 and 5204, to introduce or revert mutations T371A and TSQF(574–577)NTGY, were performed using Kunkel's automated method (22, 23) following production of single-stranded plasmids. In addition, replacement of residues 490–570 of 4790-PBP1a by the corresponding residues from 5245-PBP1a, was performed by employing a two-step PCR strategy. Three fragments were amplified: the region of 4790-PBP1a N-terminal to the target region, the zone C-terminal to the target region, and the 490–570 region of 5245-PBP1a. The three fragments were combined in a second PCR experiment, and introduced as a BamHI/XhoI fragment into modified pGEX-4T1-f1 (in which a BamHI site had been removed). All clones were verified by double-stranded sequencing (Cogenics Genome Express, Grenoble).

Protein Expression and Purification—PBP1a variants were produced by employing the same methodology used for PBP1a from strain R6 (18), albeit in this work protein expression was performed in *Escherichia coli* MC1061 cells grown in autoinduction medium (24) complemented with 100 mg·liter^{-1} of ampicillin, initially for 3 h at 37 °C and subsequently for 21 h at 20 °C. After similar lysis, centrifugation, and glutathione affinity steps, PBP1a variants were purified on a HiLoad 16/60 Superdex 200 gel filtration column (GE Healthcare) equilibrated with 10 mM sodium phosphate, pH 7.0, and 0.2 M KCl. Yields were between 4 and 12 mg per liter of culture, depending on the variant. Purity was greater than 95% as judged by Coomassie-stained SDS-PAGE.

Crystallization and Data Collection—5204-PBP1a* was prepared for crystallization trials by initial digestion the GST-PBP1a fusion protein with a 1:1000 trypsin:protein ratio for 1 h. The asterisk denotes the proteolyzed form used for crystallization, corresponding mostly to the TP domain. The resulting protein, which consists of two associated peptides (residues 47–70 and 264–653), was subsequently purified from the GST tag with a second glutathione chromatography step, which was followed by anion exchange chromatography (MonoQ HR 5/5) in 50 mM Tris-HCl, pH 8.0, 1 mM EDTA. After elution of the protein with a linear gradient to 0.5 M NaCl, 5204-PBP1a* was loaded onto a gel filtration column (Superdex 200, GE Healthcare) in 20 mM HEPES pH 7.0 and 0.1 M NaCl. Protein-containing fractions were pooled and concentrated to 4 mg/ml prior to crystallization.

The homogeneity and identity of the sample were verified by SDS-PAGE and electrospray mass spectrometry using a Q-TOF Micro spectrometer (Micromass, Manchester, UK) with an electro-spray ion source operated with a needle voltage of 3 kV, and sample cone and extraction voltages of 55 and 2 V, respectively. Spectra were recorded in the 500–2100 range of mass-to-charge (m/z) ratios. The sample was infused at 1 μM by diluting the sample in H_2O/CH_3CN (1/1 v/v), 0.2% formic acid. The data are treated by the Masslynx software (Waters). Measured masses were 2635.3 $\pm$ 0.2 Da and 43401 $\pm$ 5 Da, corresponding to the tryptic fragments 47–70 (predicted m = 2635 Da) and 264–653 (predicted m = 43395 Da).

Crystals appeared in a variety of conditions in pH values ranging from 5.5 to 8.5 with different precipitants (PEG, $(NH_4)_2SO_4$, NaCl). The best crystals were prepared in 0.1 M MES pH 6.0, 21% PEG 6000, 17 mM $BaCl_2$ at 15 °C. Crystals were cryo-cooled after sequential transfer into crystallization solutions containing increasing amounts of ethylene glycol, until a maximum value of 20%. A dataset was collected to 1.9 Å at the European Synchrotron Radiation Facility (ESRF-Grenoble) ID14-EH3 beamline at 0.931 Å. Data processing was carried out with XDS (25). The crystal structure was solved by molecular replacement using AMoRE (26) by employing the structure of PBP1a* from strain R6 as a model (PDB code 2C6W) in which active site residues were removed in order to avoid bias, and all residues differing between the two proteins were replaced by alanines. Refinement with REFMAC and CNS (27, 28), which included energy minimization, temperature factor refinement, and simulated annealing steps, was intercalated with iterative cycles of manual model building in COOT. Water

TABLE 1
Data collection and refinement

Data collection	
Space group	C2
a (Å)	122.9
b (Å)	67.0
c (Å)	49.1
β (°)	100.9
Resolution limits (Å)	19.7-1.9
Total number of reflections	23,917
Number of unique reflections	6,200
Completeness (%)	96.1 (93.2)[a]
R_{sym} (%)	11.7 (36.8)
$I/\sigma(I)$	11.1 (4.0)
Refinement	
R-factor(%)	21.2
R-free(%)	25.1
No. protein atoms	2,985
No. of water molecules	203
No. barium ions	1
Mean B factor (Å^2)	13.1
R.m.s.d from ideal geometry	
Bond lengths (Å)	0.006
Bond angles (°)	1.3

[a] The numbers in parentheses represent the values for the highest resolution shell.

molecules (203) were added to the structure using ARP/warp (29) in combination with REFMAC. MES and Ba^{2+} ions were added manually in COOT. Model quality was assessed with PROCHECK (30). Data collection and refinement statistics are included in Table 1.

Cavity Calculations—The cavity localization and volumes present in PBP1a* proteins from strains R6 and 5204 were calculated using the SURFNET program (31). The calculations were carried out in the absence of water molecules, and a sphere of radius of 1.5 Å was used.

Acylation Efficiencies—The k_2/K parameter was measured by following the decrease of the intrinsic fluorescence of the proteins (32), at various concentrations of a large excess of antibiotic, using a SFM-400 stopped-flow apparatus (Bio-Logic). Measurements were performed at 37 °C in a 100 mM sodium phosphate, pH 7.0 buffer with 0.6 μM protein and 50–1000 μM of penicillin G or cefotaxime. The excitation wavelength was 280 nm, and the emission was measured above 305 nm using a cut-off filter. The apparent pseudo-first order rate constant k_{app} was determined by non-linear fitting of the fluorescence data to equation $Fluo_t = Fluo_0 \cdot \exp(-k_{app} \cdot t) + a \cdot t + c$ using the Bio-Kine software (Bio-Logic), where the $a \cdot t + c$ accounts for the slightly drifting fluorescence signal at the end of the reaction. The efficiency of acylation k_2/K was determined by least squares linear fitting to the equation $k_{app} = (k_2/K) \cdot [\text{antibiotic}]$ with Kaleidagraph (Synergy Software, Reading, PA).

The mosaic variants of PBP1a showed no change of intrinsic fluorescence upon binding of penicillin G. Thus, the pseudo first-order rate constant for the acylation of the mosaic protein by penicillin G was measured by direct competition with cefotaxime (33). In these cases, $k_{app}(\text{penG}) = k_{app}(\text{mixture}) - k_{app}(\text{CTX})$, where $k_{app}(\text{penG})$ is the apparent rate of the reaction with penicillin G at the concentration of this antibiotic in the mixture, $k_{app}(\text{mixture})$ is the rate constant measured with a mixture of penicillin G and cefotaxime and $k_{app}(\text{CTX})$ is the rate constant measured in the absence of penicillin G but with the same concentration of cefotaxime as that present in the mixture.

Transformations and Minimal Inhibitory Concentrations—The non-encapsulated *S. pneumoniae* R6 strain was used as a recipient for genetic transformation with 5204-*pbp2x* and various *pbp1a* variants. To prevent correction of the introduced mutations by the Hex mismatch repair system of the bacteria, an altered R6 strain (*hexA::spc*) (34) was used when point mutations were introduced. Transformation and measurements of minimal inhibitory concentrations by E-tests were performed as described previously (20).

RESULTS

Sequence Comparisons—As with other low-affinity PBPs of clinical origin, the mosaicity of PBP1a defies attempts at phylogenetic-like classification. However, it appears that, with a single exception, the mosaic PBP1a sequences all share a common block of substitutions spanning residues 540–612, which includes between 10 and 18 substitutions. This sequence block is characterized by the four consecutive substitutions at positions 574–577 that were found to be important for resistance (19). This ubiquitous sequence block is combined in various ways with a variety of other blocks. The only mosaic sequence that does not contain the above-mentioned sequence block is entirely devoid of substitution in its C-terminal part following position 533.

In the course of sequencing the PBPs of 23 pneumococcal clinical isolates from the University Hospital in Grenoble, we encountered four distinct groups of mosaic PBP1a sequences, represented by strains 5204, 4790, 5245, and 5259. An alignment of the sequences corresponding to the TP domains of these PBPs is shown in Fig. 1. Sequences from strains 5204, 4790, and 5245 are very similar, and carry 45, 46, and 52 substitutions in the TP domain, respectively, with respect to PBP1a from drug-sensitive strain R6. They are from resistant strains with MIC_{penG} values ≥ 1.5 $\mu g \cdot ml^{-1}$, and carry the TSQF(574–577)NTGY substitutions within the 540–612 sequence block, as well as the T371A substitution within the first catalytic motif, next to the active site Ser^{370}. Seven substitutions near the C terminus of the TP domain are absent in 5204-PBP1a and present in PBP1a from strains 4790 and 5245. 4790-PBP1a differs from the two other close sequences by the absence of 9 substitutions, an additional one and a different one in the 495–570 segment.

PBP1a from strain 5259 is unusual in that it lacks the T371A substitution, and has no substitution following residue 533, thus lacking the abovementioned mutations in residues 574–577. The TP domain of 5259-PBP1a nevertheless carries 33 mutations, including 24 that are in common with 5204- and 5245-PBP1a. The originating strain 5259 has only a mildly reduced susceptibility to penicillin G (MIC_{penG} = 0.19 $\mu g \cdot ml^{-1}$). These four clinical variants of PBP1a, and that from the reference susceptible strain R6, gave us the opportunity to test the impact of their differences on β-lactam resistance.

Functional Characterization of PBP1a from Clinical Variants—The recombinant extracellular domains of PBP1a variants from strains R6, 5259, 4790, 5204, and 5245 were produced as GST fusion proteins, and the kinetics of the reaction of each fusion protein with penicillin G and cefotaxime were measured by following the decrease of intrinsic fluorescence that follows

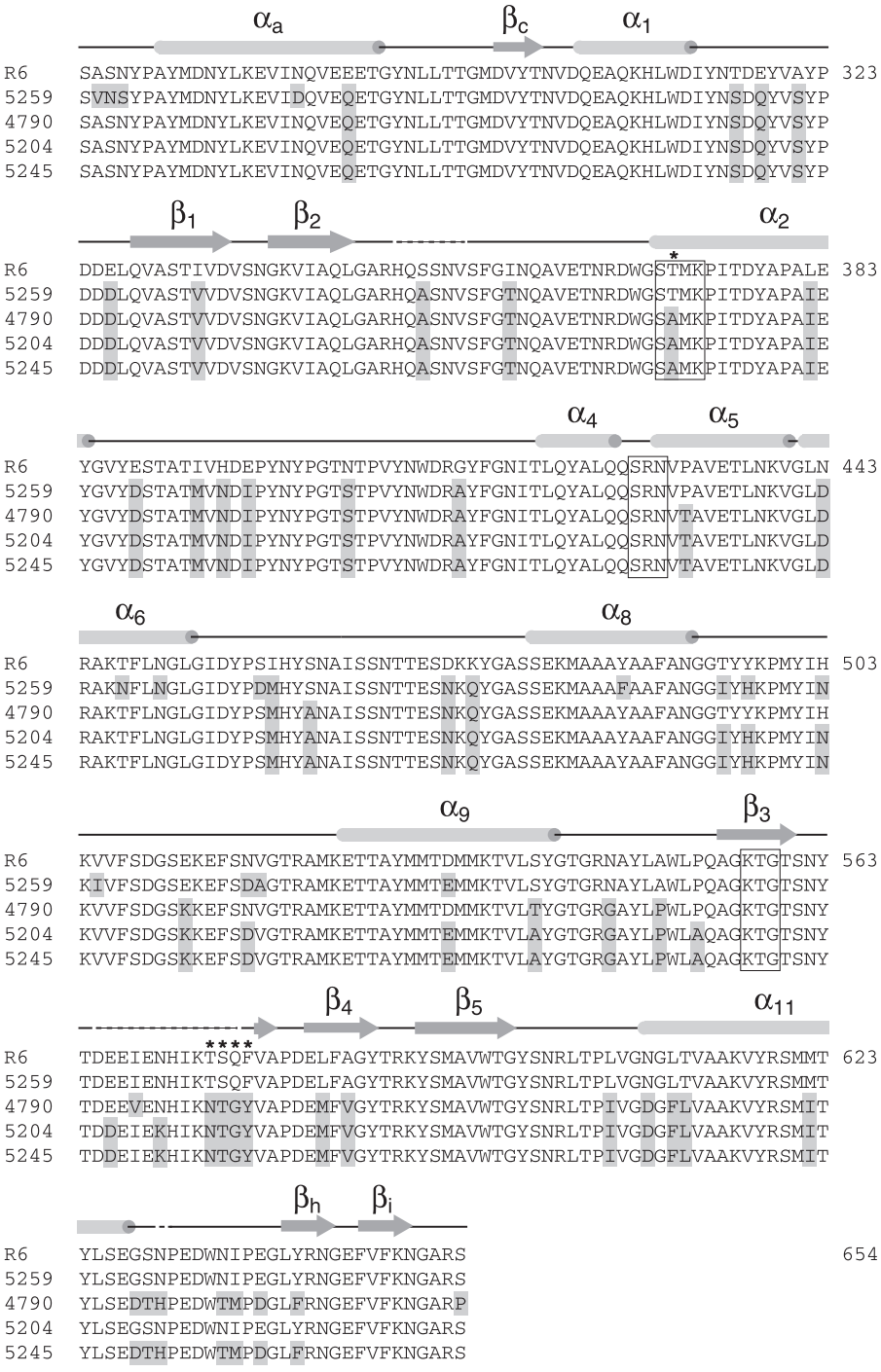

FIGURE 1. **Alignment of the sequences of segment 264–654 of PBP1a from the β-lactam-susceptible strain R6 and four β-lactam-resistant strains.** The transpeptidase domain spans residues 304–627, from α1 to α11 included. Residues differing from R6-PBP1a are *shaded*, catalytic motifs are *boxed*, positions investigated in this study are marked with an *asterisk*. Elements of secondary structure are aligned on *top* of the sequences. *Dashed lines* identify regions that were not observed in the crystal structure.

binding of the antibiotic. The reaction between PBPs and β-lactams is classically described by Reaction 1,

$$E + I \underset{}{\overset{K^{-1}}{\rightleftharpoons}} EI \xrightarrow{k_2} EI^* \xrightarrow{k_3} E + P$$

REACTION 1

where E is the enzyme, I is the β-lactam, and EI is a non-covalent complex with the dissociation constant K. The covalent acyl-enzyme EI* is formed with the rate constant k_2, and finally the enzyme is deacylated with the rate constant k_3, to regenerate an active enzyme and release an inactivated compound P. The measured acylation efficiencies, characterized by the second order rate constant k_2/K are presented in Table 2.

The values of k_2/K obtained with R6-PBP1a are consistent with previously published results (32). Mosaic PBP1a proteins have decreased acylation efficiencies by factors of 3 to 25 for cefotaxime, and 8 to 164 for penicillin G. Thus, the alterations in our variants of PBP1a have a greater effect decreasing the reactivity toward penicillin than toward cefotaxime, a cephalosporin. The acylation efficiencies of 5204- and 5245-PBP1a do not differ significantly, indicating that the seven additional substitutions of 5245-PBP1a at the C-terminus of the TP domain are not involved in the low-affinity for β-lactams. The k_2/K of 5245-PBP1a for cefotaxime and penicillin G are 1.6- and 2-fold smaller than those of 4790-PBP1a, implying that the differences at 10 positions in the 490–570 region also have a rather limited effect on the reactivity toward β-lactams. The combined effect of the 34 substitutions within the 5259-PBP1a transpeptidase domain, which do not include neither the highly prevalent TSQF(574–577)NTGY substitutions nor the active site T371A mutation, is modest but significant, indicating that mutations other than the aforementioned substitutions can also participate in the decreased affinity of PBP1a for β-lactams.

To associate the kinetic observations and the *in vivo* resistance phenomenon, the four *pbp1a* genes of clinical origin were introduced into the susceptible recipient strain R6. In order to reveal the effect of mosaic *pbp1a* genes, and because of the fact that a low affinity PBP1a is incapable of conferring resistance on its own, a fact which is linked to the essential nature and high affinity of R6-PBP2x for cefotaxime, it was necessary to co-transform *pbp1a* variants together with 5204-*pbp2x*, which

TABLE 2

Acylation efficiencies of, and resistance conferred by, PBP1a variants of clinical origins

Reactions were performed at 37 °C in 100 mM sodium phosphate, pH 7, and 0.2 M KCl. Rate constants are given with the standard error calculated from two independent experiments with five measurements of k_{app} each. The susceptible strain R6 ($MIC_{CTX} < 0.016$ $\mu g \cdot ml^{-1}$) was cotransformed with 5204-*pbp2x*.

PBP1a	k_2/K		MIC Cefotaxime
	Penicillin G	Cefotaxime	
	$M^{-1} \cdot s^{-1}$		$\mu g \cdot ml^{-1}$
R6	69000 ± 15000	11000 ± 700	0.25
5259	8600 ± 600	4000 ± 550	0.38
4790	820 ± 160	700 ± 10	0.75
5204	430 ± 110	480 ± 7	1
5245	420 ± 90	440 ± 40	1

TABLE 3

Acylation efficiencies of, and resistance conferred by, PBP1a point-mutants

Reactions were at 37 °C in 100 mM sodium phosphate, pH 7, and 0.2 M KCl. Rate constants are given with the standard error calculated from two independent experiments with five measurements of k_{app} each. The susceptible strain R6 ($MIC_{CTX} < 0.016$ $\mu g \cdot ml^{-1}$) was cotransformed with 5204-*pbp2x*.

PBP1a	k_2/K		MIC Cefotaxime
	Penicillin G	Cefotaxime	
	$M^{-1} \cdot s^{-1}$		$\mu g \cdot ml^{-1}$
R6			
Wild type	69000 ± 15000	11000 ± 700	0.25
T371A	2640 ± 150	4600 ± 210	NT[a]
TSQF(574–577)NTGY	1420 ± 210	2000 ± 40	NT
T371A/TSQF(574–577)NTGY	1330 ± 145	1140 ± 30	0.38
5204			
Wild type	430 ± 110	480 ± 7	1
A371T	2080 ± 550	850 ± 30	0.5
NTGY(574–577)TSQF	750 ± 90	1210 ± 60	0.75
A371T/NTGY(574–577)TSQF	3200 ± 440	1400 ± 80	0.5

[a] NT, no transformants were isolated with a resistance to cefotaxime greater than that conferred by 5204-*pbp2x* alone.

encodes a PBP2x with a very low affinity for cephalosporins (20). The other pneumococcal PBPs are either non-essential, or, as in the case of PBP2b, have a naturally low affinity for cephalosporins. Therefore, resistance to cefotaxime can be conferred by altering only *pbp2x* and *pbp1a*. The MIC value for cefotaxime was measured and results are given in Table 2. The PBP1a proteins with the lowest k_2/K confer the highest resistance levels. Interestingly, even the modestly decreased efficiency of acylation of 5259-PBP1a increases the resistance level.

Role of the T371A and TSQF(574–577)NTGY Mutations—The TSQF(574–577)NTGY block of mutations has been shown to be an important determinant of the level of resistance conferred by PBP1a from strain 3191 (19). Another potentially important substitution is T371A, which lies adjacent to Ser^{370}, the active site nucleophile; notably, the same substitution is observed in many mosaic PBP2x variants and has been shown to influence the acylation efficiency of this latter protein (35). To evaluate the impact of these mutations on the reactivity of PBP1a toward β-lactams, a set of six variants were constructed, where the T371A and TSQF(574–577)NTGY mutations were introduced individually or together into R6-PBP1a. The reverse substitutions were also introduced into 5204-PBP1a. The recombinant extracellular domains fused to GST were produced, and their efficiencies of acylation by cefotaxime and penicillin G were measured (Table 3).

The T371A substitution diminishes the efficiency of acylation of R6-PBP1a by cefotaxime (2.4-fold), and particularly by penicillin G (26-fold). Conversely, reversion of the substitution at position 371 in 5204-PBP1a from A to T increases the k_2/K (1.8- and 4.8-fold for cefotaxime and penicillin G, respectively). The impact of the TSQF(574–577)NTGY mutations on the acylation efficiency of R6-PBP1a is even greater with decreases of 5.5- and 49-fold for cefotaxime and penicillin G, respectively. The introduction of reciprocal mutations (NTGY(574–577)TSQF) in 5204-PBP1a increases the k_2/K by factors of 2.5 and 1.7, respectively. The combined effect of the two sets of mutations at positions 371 and 574–577 is greater than the individual mutations, both in R6-PBP1a and in 5204-PBP1a. It is of note that the effect of the direct mutations in R6-PBP1a is larger, particularly regarding the reaction with penicillin G, than that of the reverse substitutions in 5204-PBP1a.

To investigate *in vivo* the effect of the point mutations, attempts were made to transform the susceptible recipient strain R6 with the six artificial *pbp1a* variants, together with the mosaic 5204-*pbp2x*. When transformants were obtained with a resistance to cefotaxime greater than that conferred by 5204-*pbp2x* alone, the MIC was measured (Table 3). The three 5204-PBP1a variants conferred increased resistance, although to a lesser extent than the wild-type 5204-PBP1a, thus confirming the importance of the TSQF(574–577)NTGY mutations and T371A substitution for the resistance process. Of the R6-PBP1a variants, only the double mutant conferred increased resistance. No transformants were obtained with the single mutants. Note that the R6-PBP1a single mutants are those with the least decreased efficiency of acylation.

It is noteworthy that the measured MICs do not correlate perfectly with the acylation efficiencies. Particularly remarkable is the fact that transformants were obtained with the 5259-*pbp1a* of clinical origin, although the encoded protein has a k_2/K for cefotaxime of 4000 $M^{-1} \cdot s^{-1}$ (Table 2), whereas no clones were selected with the R6-*pbp1a* TSQF(574–577)NTGY variant, despite the lower efficiency of acylation of the encoded PBP1a ($k_2/K = 2000$ $M^{-1} \cdot s^{-1}$).

Absence of Influence of Mutations Outside of the Transpeptidase Domain—It has generally been assumed that substitutions outside of the TP domain of the PBPs are neutral regarding the acylation by β-lactams. To test this assumption in the case of PBP1a, we exchanged region 490–570 of 4790-PBP1a for the corresponding region from 5245-PBP1a. This exchange resulted in a protein termed Hybrid-PBP1a, which has a transpeptidase domain identical to that of 5245-PBP1a. However, Hybrid- and 5245-PBP1a differ at 14 positions outside of the transpeptidase domain, 4 in the glycosyltransferase domain and 10 in the C-terminal region. The measured acylation efficiencies by cefotaxime and penicillin G were 405 ± 62 M^{-1} s^{-1} and 440 ± 90 M^{-1} s^{-1}, respectively. These values are similar to those measured with 5245-PBP1a (Table 2). The MIC of cefotaxime for R6 *S. pneumoniae* transformed with Hybrid-*pbp1a* and 5204-*pbp2x* (1 $\mu g \cdot ml^{-1}$) was the same as that obtained with 5245-*pbp1a* and 5204-*pbp2x*.

Overall Fold of PBP1a (5204)*—The crystal structure of 5204-PBP1a*, solved by molecular replacement using PBP1a* from strain R6 as a model, is remarkable in its resolution (1.9 Å), which is considerably higher than that of R6-PBP1a* (2.6 Å;

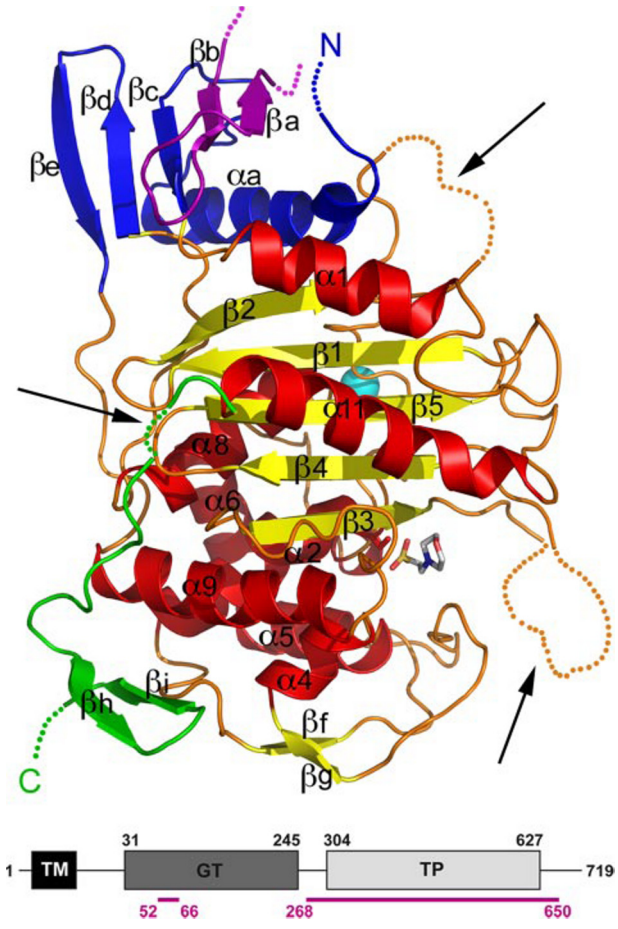

FIGURE 2. **Overall structure of a soluble form of PBP1a from *S. pneumoniae* β-lactam-resistant strain 5204.** The full TP domain (residues 304–627, in *red* and *yellow*) is flanked by a small C-terminal domain (in *green*) and an N-terminal interdomain linker (in *blue*). A small peptide of the GT domain (residues 52–66, in *violet*) remains associated with the TP domain. The regions, that could not be traced in the electron density map are marked with *dotted lines* pointed with *arrows*. The active side Ser^{370} and the MES molecule are shown in *sticks*, the Ba^{2+} ion is shown as a *cyan sphere*. *Bottom*, numbering scheme for the different domains, and in *magenta* the region present in the structure.

(18)). Briefly, the structure consists of three major regions (Fig. 2): a central TP domain (residues 304–627) composed of 5 antiparallel β strands (β1-β5) surrounded by α-helices; a linker region (residues 268–303), which serves as structural intermediary between GT and TP domains; part (Ser^{52}–Leu^{66}) of a small peptide (residues 47–70) of the GT domain, which remains associated to the TP domain during the purification; and a small C-terminal domain (from Gly^{628} to Asn^{650}). The structural superposition of PBP1a* variants from strains 5204 and R6 shows an r.m.s. deviation of 0.5 Å (considering 348 Cα atoms). The main differences involve loop regions within the 5204-PBP1a* structure, which are not visible in the electron density map, namely in three distinct regions (*broken lines* in Fig. 1): loop 350–354, which includes the S351A mutation (*orange dots* in Fig. 2); the loop spanning Asp^{566} to Gly^{576} (*orange dots* in Fig. 2), and residue Asn^{630} (*green dots* in Fig. 2). In addition, the present structure includes a Ba^{2+} ion, as well as a molecule of MES (included in the crystallization buffer). The Ba^{2+} ion is stabilized within PBP1a* by a network of interactions, which include the backbone carbonyl and Oγ atoms of Ser^{475} and Thr^{364}, the backbone carbonyls of Asn^{473} and Tyr^{476}, and three water molecules. The sulfate group of the MES molecule is hydrogen-bonded to the active site Oγ-Ser^{370}, Oγ-Ser^{428}, Oγ-Thr^{560}, Oγ-Thr^{558}, and one water molecule. Interestingly, the MES sulfate group occupies an analogous position to a sulfate ion in structures of PBP2x (PDB:1QME and 1RP5), and is also positioned similarly to the carboxyl group of cefotaxime in the structure of R6-PBP1a* complexed with this antibiotic (PDB: 2C5W)(Fig. 4).

The 5204-PBP1a Active Site*—The active site of 5204-PBP1a* is delineated by the three conserved motifs found in β-lactam-recognizing enzymes: S*X*X*K* (Ser^{370}-*X*-*X*-Lys^{373}), which includes the catalytic serine, S*X*N (Ser^{428}-*X*-Asn^{430}), on the loop between α4 and α5, and KTG (Lys^{557}-Thr^{558}-Gly^{559}), along β3. A superposition of the active sites of PBP1a* from strains R6 and 5204 reveals that, although the positions of catalytic residues on β3 are conserved, the active site of the enzyme from the drug-resistant strain shows key modifications, which mostly affect the hydrogen bonding network (Fig. 3). Notably, the interaction between Asn^{430} and the backbone carbonyl of Tyr^{409} is lost, while a new hydrogen bond is formed with the catalytic Lys^{373}. In addition, Asn^{562}, present in the loop between β3 and β4, points to the interior of the active site, thus participating in the restriction of the entry into the catalytic cleft (Fig. 3). It is of interest that the nucleophilic Ser^{370}, which in the structure of the enzyme from strain R6 pointed into the active site, in the present structure points way from it, toward β3, interacting both with the backbone amino group of Thr^{560} and a carbonyl group of the MES molecule.

The only mutation that lies in the vicinity of the PBP1a* active site is T371A. In the R6-PBP1a* structure, the Oγ-Thr^{371} atom forms a hydrogen bond with the backbone carbonyl group of Trp^{368}; in 5204-PBP1a*, this interaction is absent. It is thus conceivable that this modification is responsible for the fact that, in 5204-PBP1a*, the catalytic serine is shifted by 0.6–1.1 Å (in relation to R6-PBP1a*, PDB codes 2C6W and 2C5W, respectively). A similar conformation for the Oγ of the catalytic serine was observed in the structures of PBP2x variants from drug-resistant strains Sp328 and 5259, and in an active site double point mutant of PBP2x (10, 20, 36).

The introduction of substitutions in R6-PBP1a at positions 574–577 is responsible for a 49-fold decrease in the acylation efficiency by penicillin G (Table 3). In PBP1a*, these residues are located in the loop between β3 and β4 (Fig. 3*A*), a region which, in other PBPs, displays high flexibility (17). In the present structure, the β3-β4 loop is untraceable in the electron density map, possibly also due to inherent flexibility. Note that prolonged incubation with trypsin resulted in secondary cleavage after Lys^{573} (as determined by mass spectometry and N-terminal sequencing), also indicative of flexibility in this region.

The only residue from the block of four mutated positions that is visible is residue Tyr^{577}. In the structure of R6-PBP1a*, Trp^{411} and Phe^{577} line the lower part of the active site cavity, generating a hydrohobic wall (18). The mutation of Phe^{577} to Tyr in 5204-PBP1a* could increase the local hydrophilicity, affecting the recognition/entrance of the antibiotic into the active site. In addition, in 5204-PBP1a*, loop 408–416, which carries Trp^{411}, is shifted by 3.5 Å in the direction of the catalytic

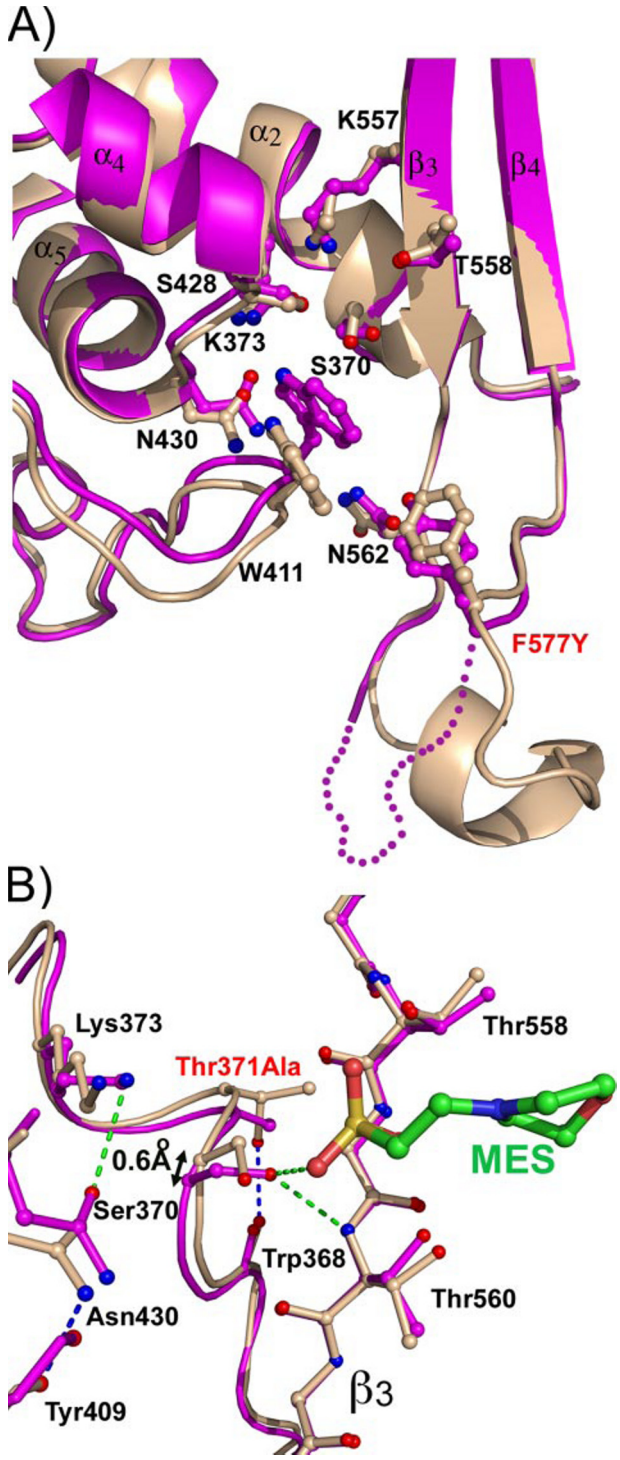

FIGURE 3. **Superposition of the two PBP1a structures from the drug-susceptible strain R6 (in *white*) and the drug-resistant strain 5204 (in *magenta*).** The residues involved in the acylation and ligand binding are shown in *panel A*. The details of the active site are shown in *panel B*. The hydrogen bonds are shown as *dashed lines* in *blue* and *green*, for R6-PBP1a and 5204-PBP1a, respectively. The MES molecule present in the 5204-PBP1a structure is shown in *green*. The residues that differ between the two proteins are labeled in *red*.

serine (Figs. 3*A* and 4). The movement of this particular loop region could be related to either of two possibilities. First, the side chain of Trp^{411} could be potentially stabilized through hydrophobic interactions with the MES molecule located in its vicinity. However, the heterocyclic indole ring of Trp^{411} and the morpholine ring of MES lie at an angle of 90° to each other (with the closest atomic distance being of 3.7 Å). A second explanation could involve the generation of contacts by loop 411–416 with a nearby symmetry mate; although this loop region is located in the proximity of a symmetry-related molecule within the crystal lattice, the closest interactions are in the range of 3.5–4.5 Å. Thus, neither of the two explanations above can fully account for the large movement observed in loop 411–416, which restricts the size of the active site cavity.

To quantify these findings, the volume of the protein cavities were calculated with the program SURFNET (31) for both PBP1a* variants. Fig. 4*C* displays a representation of the cavities within the active sites of both enzymes from drug-susceptible and -resistant strains. Using this methodology, it is clear that the cavity of 5204-PBP1a* is not only smaller than that of R6-PBP1a*, but is also discontinuous, because in particular of the orientation of Tyr^{577}.

DISCUSSION

S. pneumoniae acquires resistance to β-lactam antibiotics by producing highly mutated PBPs. PBP1a, a bifunctional enzyme, plays a key role in this process, because only when this enzyme has been mutated (in addition to PBP2x and PBP2b) can the bacterium express high levels of resistance to β-lactams (13–16). The present study demonstrates that the resistance conferred by key substitutions found in clinical resistant strains is indeed correlated with an impaired efficiency of acylation by antibiotics, most probably because of restricted access of the antibiotic to the active site cavity.

Analysis of PBP1a variants from different clinical drug-resistant strains reveals that a single mutation, T371A, as well as a block of mutations spanning residues 574–577, are conserved among a variety of strains, and have an important impact on the reaction of PBP1a with β-lactams (Tables 2 and 3 and Ref. 19). The high resolution crystal structure of PBP1a* from a pneumococcal strain with very high resistance to β-lactams, presented here, shows the active site to be greatly affected by the T371A mutation, because the loss of a hydrogen bond, which is clearly present in the R6-PBP1a* structure between Thr^{371} and the backbone of Trp^{368}, causes a significant shift in the position of the catalytic serine. In addition, the active site is clearly restricted, not only due to the movement of Asn^{562} and the loop carrying Trp^{411}, but also to the fact that Tyr^{577}, a residue which is located on the loop which connects β3 and β4 and which is at the end of the TSQF(574–577)NTGY mutation block, points toward the entrance of the cleft. Tyr^{577} is 2 Å closer to the active site serine than the corresponding residue in PBP1a* from drug-sensitive strain R6 (Phe^{577}). It is of note that this particular mutation slightly modifies the hydrophilicity of the entry of the active site and could interfere with antibiotic binding, therefore partially accounting for the decrease in acylation efficiency observed for the single mutation in region 574–577. Due to the high flexibility of the rest of the corresponding loop (as indicated by the absence of electron density for this region in the map, and the relative sensitivity of this region to proteolysis, not shown), the structural implication of the other 3 important mutations (T574N-S575T-Q576G) in the resistance phenome-

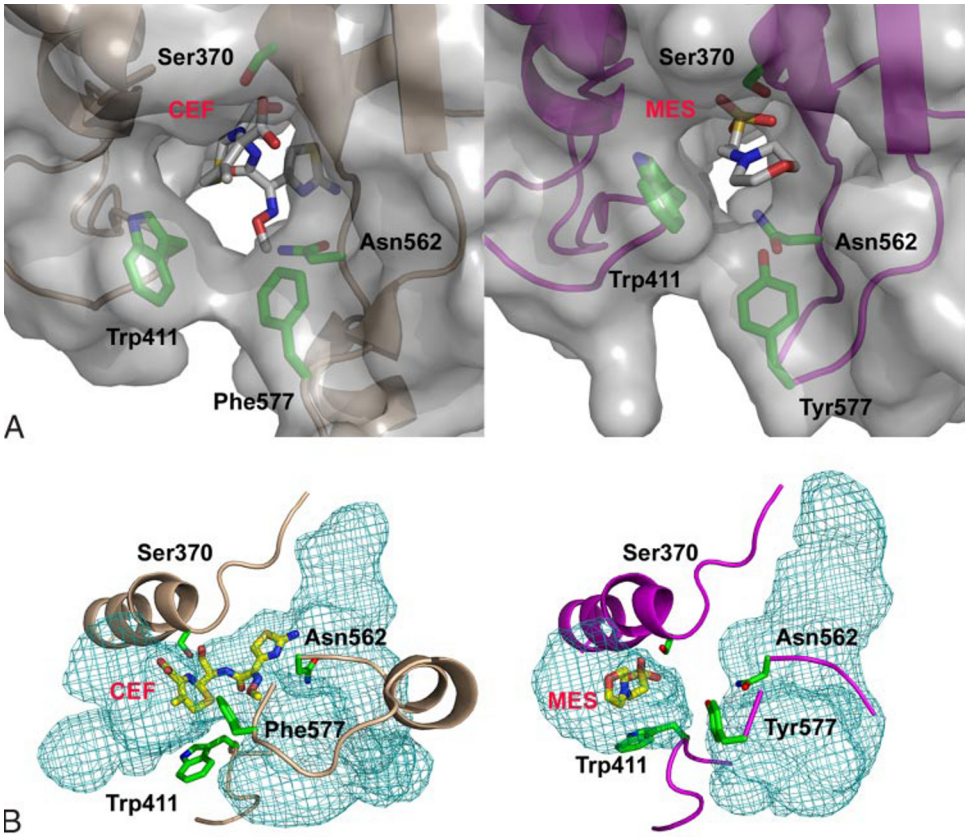

FIGURE 4. **Active sites comparison between PBP1a from strain R6 (*left*) and strain 5204 (*right*).** *Panel A* shows the protein surfaces and *panel B* the cavities present in both active sites (shown as *meshes*). The residues involved in active site restriction, as well as the cefotaxime molecule in the R6 structure, and the MES molecule in the 5204 structure are shown as *sticks*.

non is not clear, but the possibility that the residues in this flexible loop could also interfere with entrance of the antibiotic into the active site cannot be excluded. Taken together, all of these observations point to the possibility that the drug resistance phenomenon brought about by mutations in 5204-PBP1a could be significantly different from the one suggested for pneumococcal PBP2x from the drug-resistant strain Sp328, in which an opening of the active site was identified (36).

It is of interest that although the T371A and TSQF(574–577)NTGY mutations have a drastic effect in reducing the reactivity of R6-PBP1a toward β-lactams, with the resulting variants retaining a rather low efficiency of acylation, the reciprocal substitutions in 5204-PBP1a do not restore a particularly high efficiency of acylation. This finding indicates that the other substitutions make a significant collective contribution to the resistance. This is supported by the fact that PBP1a from pneumococcal strain 5259 displays reduced reactivity toward β-lactams and confers some resistance, despite lacking the T371A and TSQF(574–577)NTGY mutations. This finding may explain why a PCR-based assay, which tests for the presence of the TSQF(574–577)NTGY mutation, fails to identify all the strains with a MIC_{CTX} lower or equal to 0.25 $\mu g \cdot ml^{-1}$ (37). The precise determination of the role of each substitution would require a substantial effort at site-directed mutagenesis and characterization, as has been performed with PBP2x (11, 23).

A puzzling observation is the fact that PBP1a variants displaying similar acylation efficiencies (k_2/K) can confer different levels of resistance. R6-PBP1a with the T371A and TSQF(574–577)NTGY mutations confers a lower resistance level than the 5204-PBP1a reciprocal mutant, which has a similar or even faster rate of acylation (Table 2). A biochemical explanation of this phenomenon could involve the role of the deacylation rate, which can be different in the two proteins. A faster deacylation rate, which regenerates an active enzyme, results in a smaller steady-state proportion of inactivated PBP at a given concentration of antibiotic. In the case of some variants of PBP2x, a faster deacylation rate, that could conceivably contribute to the resistance phenotype, has been measured (20, 38). An alternative explanation is that despite having similar rates of acylation by β-lactams, the two considered PBP1a variants may not function physiologically with the same efficacy. The 5204-PBP1a variant could fare better with its physiological substrates to build the peptidoglycan due to compensatory mutations, whereas R6-PBP1a could have its enzymatic function severely affected by the point mutations. Such a difference could possibly result in different levels of resistance.

This latter explanation points to a central ambiguity in the study of PBPs that have a low affinity for β-lactams. These antibiotics are thought to mimic the natural substrate, yet altered PBPs can discriminate β-lactams from physiological D-Ala-D-Ala-bearing substrates. To combat resistance, we will need to understand not only how the reactivity with the antibiotic is affected, but also how normal activity is maintained.

Acknowledgments—We thank David Lemaire for mass spectrometry analysis, Jean-Pierre Andrieux for N-terminal sequencing, Carlos Contreras-Martel for performing SURFNET calculations, and Otto Dideberg for suggestions and critical reading of the manuscript.

REFERENCES

1. Maugein, J., Croizé, J., Ros, A., Bourdon, S., Brun, M., Cattier, B., Chanal, C., Chabanon, G., Chardon, H., Chomarat, M., Coignard, B., Demachy, M.-C., Donnio, P.-Y., Dupont, P., Fosse, T., Gravet, A., Grignon, B., Laurans, G., Péchinot, A., Ploy, M.-C., Roussel-Delvallez, M., Thoreux, P.-H., Varon, E., Vergnaud, M., Vernet-Garnier, V., and Weber, M. (2006) *Bulletin Epidémiologique Hebdomadaire* **1**, 6–8
2. Tipper, D. J., and Strominger, J. L. (1965) *Proc. Natl. Acad. Sci. U. S. A.* **54,** 1133–1141
3. Hakenbeck, R., Grebe, T., Zahner, D., and Stock, J. B. (1999) *Mol Microbiol* **33,** 673–678
4. Dowson, C. G., Hutchison, A., Brannigan, J. A., George, R. C., Hansman, D., Linares, J., Tomasz, A., Smith, J. M., and Spratt, B. G. (1989) *Proc. Natl.*

Acad. Sci. U. S. A. **86,** 8842–8846
5. Laible, G., Spratt, B. G., and Hakenbeck, R. (1991) *Mol. Microbiol.* **5,** 1993–2002
6. Martin, C., Sibold, C., and Hakenbeck, R. (1992) *EMBO J.* **11,** 3831–3836
7. Dowson, C. G., Coffey, T. J., Kell, C., and Whiley, R. A. (1993) *Mol. Microbiol.* **9,** 635–643
8. Sibold, C., Henrichsen, J., Konig, A., Martin, C., Chalkley, L., and Hakenbeck, R. (1994) *Mol. Microbiol.* **12,** 1013–1023
9. McGee, L., McDougal, L., Zhou, J., Spratt, B. G., Tenover, F. C., George, R., Hakenbeck, R., Hryniewicz, W., Lefevre, J. C., Tomasz, A., and Klugman, K. P. (2001) *J. Clin. Microbiol.* **39,** 2565–2571
10. Pernot, L., Chesnel, L., Le Gouellec, A., Croize, J., Vernet, T., Dideberg, O., and Dessen, A. (2004) *J. Biol. Chem.* **279,** 16463–16470
11. Carapito, R., Chesnel, L., Vernet, T., and Zapun, A. (2006) *J. Biol. Chem.* **281,** 1771–1777
12. Grebe, T., and Hakenbeck, R. (1996) *Antimicrob. Agents Chemother.* **40,** 829–834
13. Barcus, V. A., Ghanekar, K., Yeo, M., Coffey, T. J., and Dowson, C. G. (1995) *FEMS Microbiol. Lett.* **126,** 299–303
14. Reichmann, P., Konig, A., Marton, A., and Hakenbeck, R. (1996) *Microb. Drug Resist.* **2,** 177–181
15. Smith, A. M., and Klugman, K. P. (1998) *Antimicrob. Agents Chemother.* **42,** 1329–1333
16. du Plessis, M., Bingen, E., and Klugman, K. P. (2002) *Antimicrob. Agents Chemother.* **46,** 2349–2357
17. Macheboeuf, P., Contreras-Martel, C., Job, V., Dideberg, O., and Dessen, A. (2006) *FEMS Microbiol. Rev.* **30,** 673–691
18. Contreras-Martel, C., Job, V., Di Guilmi, A. M., Vernet, T., Dideberg, O., and Dessen, A. (2006) *J. Mol. Biol.* **355,** 684–696
19. Smith, A. M., and Klugman, K. P. (2003) *Antimicrob. Agents Chemother.* **47,** 387–389
20. Chesnel, L., Pernot, L., Lemaire, D., Champelovier, D., Croize, J., Dideberg, O., Vernet, T., and Zapun, A. (2003) *J. Biol. Chem.* **278,** 44448–44456
21. Mouz, N., Di Guilmi, A. M., Gordon, E., Hakenbeck, R., Dideberg, O., and Vernet, T. (1999) *J. Biol. Chem.* **274,** 19175–19180
22. Kunkel, T., Bebenek, K., and McClary, J. (1991) *Methods Enzymol.* **204,** 125–139
23. Carapito, R., Gallet, B., Zapun, A., and Vernet, T. (2006) *Anal. Biochem.* **355,** 110–116
24. Studier, F. W. (2005) *Protein Expr. Purif.* **41,** 207–234
25. Kabsch, W. (1993) *J. Appl. Crystallogr.* **26,** 795–800
26. Navaza, J. (2001) *Acta Crystallogr. Sect. D* **57,** 1367–1372
27. Collaborative Computing Program Number 4 and Collaborative Computing Project for NMR (1994) *Acta Crystallogr. Sect. D Biol. Crystallogr.* **50,** 760–766
28. Brünger, A. T., Adams, P. D., Clore, G. M., DeLano, W. L., Gros, P., Grosse-Kunstleve, R. W., Jiang, J. S., Kuszewski, J., Nilges, M., Pannu, N. S., Read, R. J., Rice, L. M., T., S., and Warren, G. L. (1998) *Acta Crystallogr. Sect. D* **54,** 905–921
29. Morris, R. J., Perrakis, A., and Lamzin, V. S. (2003) *Methods Enzymol.* **374,** 229–244
30. Laskowski, R. A., MacArthur, M. W., Moss, D. S., and Thornton, J. M. (1993) *J. Appl. Crystallogr.* **26,** 283–291
31. Laskowski, R. A. (1995) *J. Mol. Graph* **13,** 323–330
32. Di Guilmi, A. M., Mouz, N., Andrieu, J. P., Hoskins, J., Jaskunas, S. R., Gagnon, J., Dideberg, O., and Vernet, T. (1998) *J. Bacteriol.* **180,** 5652–5659
33. Graves-Woodward, K., and Pratt, R. F. (1998) *Biochem. J.* **332,** 755–761
34. Claverys, J. P., and Lacks, S. A. (1986) *Microbiol. Rev.* **50,** 133–165
35. Mouz, N., Gordon, E., Di Guilmi, A. M., Petit, I., Petillot, Y., Dupont, Y., Hakenbeck, R., Vernet, T., and Dideberg, O. (1998) *Proc. Natl. Acad. Sci. U. S. A.* **95,** 13403–13406
36. Dessen, A., Mouz, N., Gordon, E., Hopkins, J., and Dideberg, O. (2001) *J. Biol. Chem.* **276,** 45106–45112
37. du Plessis, M., Smith, A. M., and Klugman, K. P. (1999) *J. Clin. Microbiol.* **37,** 628–632
38. Lu, W. P., Kincaid, E., Sun, Y., and Bauer, M. D. (2001) *J. Biol. Chem.* **276,** 31494–31501